

General Disclaimer

One or more of the Following Statements may affect this Document

- This document has been reproduced from the best copy furnished by the organizational source. It is being released in the interest of making available as much information as possible.
- This document may contain data, which exceeds the sheet parameters. It was furnished in this condition by the organizational source and is the best copy available.
- This document may contain tone-on-tone or color graphs, charts and/or pictures, which have been reproduced in black and white.
- This document is paginated as submitted by the original source.
- Portions of this document are not fully legible due to the historical nature of some of the material. However, it is the best reproduction available from the original submission.

**NASA TECHNICAL
MEMORANDUM**

NASA TM X-71784

NASA TM X-71784

(NASA-TM-X-71784) SIDE CRACKED PLATED
SUBJECT TO COMBINED DIRECT AND BENDING
FORCES (NASA) 21 p HC \$3.25 CSCL 20K

N75-30605

Unclas
34274

G3/39

**SIDE CRACKED PLATES SUBJECT TO
COMBINED DIRECT AND BENDING FORCES**

by John E. Srawley and Bernard Gross
Lewis Research Center
Cleveland, Ohio 44135

TECHNICAL PAPER to be presented at
Ninth Symposium on Fracture Mechanics
sponsored by the American Society for Testing
and Materials
Pittsburgh, Pennsylvania, August 25-27, 1975



SIDE CRACKED PLATES SUBJECT TO COMBINED DIRECT AND BENDING FORCES

John E. Srawley and Bernard Gross

National Aeronautics and Space Administration
Lewis Research Center
Cleveland, Ohio

ABSTRACT

The opening mode stress intensity factor and the associated crack mouth displacement are comprehensively treated using planar boundary collocation results supplemented by end point values from the literature. Data are expressed in terms of dimensionless coefficients of convenient form which are each functions of two dimensionless parameters, the relative crack length, and a load combination parameter which uniquely characterizes all possible combinations of tension or compression with bending or counterbending. Accurate interpolation expressions are provided which cover the entire ranges of both parameters. Application is limited to specimens with ratios of effective half-height to width not less than unity.

LIST OF SYMBOLS

- a crack length (or depth); see Fig. 1
- B specimen thickness; see Fig. 1
- c_1, c_2 numerical coefficients in Eqn. (11)
- E Young's modulus
- E' effective modulus; see Discussion
- H effective half-height of specimen
- K stress intensity factor (Mode I in this context)
- M moment of complementary couple
- P resultant applied force
- s distance of knife edge from crack mouth (see Crack Mouth Displacement Slopes)
- v crack mouth displacement
- W specimen width; see Fig. 1

- α relative crack length, a/W
 Γ dimensionless stress intensity coefficient
 Δ dimensionless crack mouth displacement coefficient
 θ displacement combination parameter, $\arctan(v_M/v_P)$
 ν Poisson's ratio
 σ stress
 ω load combination parameter, $\arctan(\sigma_M/\sigma_P)$

Subscripts:

- I opening mode of crack tip deformation
M value for net section bending ($\omega = 1$)
P value for net section tension ($\omega = 0$)

1. INTRODUCTION

This paper is a comprehensive treatment of the opening mode stress intensity factor, K_I , and the associated crack mouth displacement, v , for quasiplanar rectangular specimens with single side cracks of any uniform depth, loaded in any manner that can be represented sufficiently well by a linear distribution of normal forces across each end boundary. To justify such a representation of simple practical methods of load application, the ratio of effective half-height to width of the specimen should not be less than unity, preferably substantially greater for higher accuracy of application of the displacement data. The treatment of shorter specimens would require more refined, nonlinear modeling of the actual loading force distribution so that the interaction with the crack stress field would be adequately approximated.

Results for certain cases covered here have been published previously by the present authors, such as in Ref. [1], and by others cited in Ref. [2]. However, these previous results are not sufficient for a comprehensive treatment of the subject. The results of this study constitute a homogeneous body of data which were subjected to linear regression analysis to estimate consistency and precision.

In this treatment the distribution of normal forces across an end boundary is characterized by the statically equivalent combination of resultant force, chosen to act through mid net section, and the complementary couple. Either the force, or the couple, or both, can act in a positive sense so as to cause the crack to open in the vicinity of the tip (tension or bending), or can act in a negative sense to cause the

crack to tend to close near the tip (compression or counterbending). For some load combinations the effect on the crack mouth is the same as at the tip; for others, such as combined tension and counterbending, it may be opposite. In general, the force and the couple are to be regarded as independent variables. Commonly, however, in practical testing, when force is applied by a single actuator, there is a proportional relation between the force and the couple which depends on the line of action of the force and on the relative crack length.

The data are given in the form of dimensionless coefficients, $\Gamma(K_I)$ and $\Delta(v)$, which are both functions of two dimensionless parameters, the relative crack length, α , and the load combination parameter, ω , equal to $\arctan(6M/P(W - a))$, where P is the magnitude of the resultant force, M that of the moment of the complementary couple, W is the specimen width, and a is the crack length. Both Γ and Δ are linear functions of the quantity $\tan(\pi/4 - \omega)$, and the coefficients of the linear equations are finitely bounded functions of α which are expressed as rational algebraic functions for interpolation purposes. The ratio H/W , of the half-height to width of the specimen is the third independent parameter which would be expected to have an appreciable effect on the values of Γ and Δ if it were less than unity. For the values considered: 1, 2, and 4, however, the effect on Γ was found to be practically negligible, and the effect on Δ erratic and of the order of 5 percent at the most.

The primary data for values of the relative crack length α other than the end points, 0 and 1, were obtained by the boundary collocation method of analysis as described in Ref. [3]; the end point values were obtained from Refs. [2] or [4] except in one case which is discussed later.

The purpose of this study is to serve as a prerequisite for the development of new test methods for measurement of such properties of materials as fracture toughness, fatigue crack propagation resistance and stress corrosion crack propagation resistance. The potential advantages of the full range of load combinations has by no means been thoroughly explored. Nor has the possibility that the property of interest might be significantly dependent on the mode of loading. This possibility follows from the fact that the crack tip plastic zone characteristics will certainly be affected.

In the application of results of planar analysis it is useful to distinguish between two types of quasi-planar practical plate specimens, as shown in cross section in Fig. 1: (a) edge-cracked, and (b) face-cracked. In either case the crack length, or depth, must be practically uniform if the planar analysis is to apply accurately. Both kinds of specimen are necessary so that tests can be conducted with cracks oriented in different directions with respect to material texture; in particular, in the direction that cracks have been found to occur in service of a structural member. One particular use of the face-cracked specimen follows from regarding it as the extreme case of the widely used part-through cracked, or surface cracked type of specimen, Fig. 1(c). The

analysis of part-through cracked specimens is essentially three-dimensional, and presents difficulties which are not yet satisfactorily resolved [5]. The present results provide a bound on the three-dimensional analysis, and are therefore a useful guide as to its accuracy. Moreover, tests of face-cracked specimens can provide a useful check on the reliability of tests of part-through cracked specimens, or serve to substitute for them when convenient.

2. BOUNDARY COLLOCATION ANALYSIS

Boundary collocation analyses were conducted for two different, but equivalent, types of end boundary conditions, as shown in Fig. 2(a). The first type is a linear distribution of normal tractions across the end boundary, as shown at the top of the figure. The second type consists of uniform distributions of shear stress along prolongations of the side boundaries, as shown at the bottom of the figure. Both distributions are statically equivalent to the combination of resultant force, P , which acts through mid net section, and complementary couple of moment M . The use of these two distinct types of boundary conditions provided a check of the consistency of the method. It was found that the same results could be obtained with either type, but that the analysis had to be carried considerably further to reach satisfactory convergence when the second (shear) type of boundary condition was used. Satisfactory convergence is approached by successive runs with increasing numbers of boundary stations until there is no significant variation in the result. The complete set of results presented here was therefore obtained with the first (normal stress) type of boundary conditions, and a substantial number of these results were confirmed with the second type. The purpose of Fig. 2(b) is to show other equivalent expressions of the load combination: a linear distribution of normal tractions across the net section; and a pair of parallel forces acting at the corners. These expressions serve conceptual purposes; they are of no concern to the boundary collocation analysis.

The boundary collocation procedure used has been described in Ref. [3], and in greater detail in Ref. [6]. Briefly, a stress function which satisfies the necessary conditions on the crack boundary surface takes the form of an infinite series with unknown coefficients. This series is truncated and the remaining coefficients are determined from the conditions that the stress function and its derivative must satisfy the imposed boundary conditions at a finite number of selected boundary stations. The derivation of the boundary values of the stress function and its derivative for the present cases are given in Appendix A. The number of undetermined coefficients can be equal to or less than twice the number of boundary stations. If it is less, then an overdetermined system of simultaneous equations results, and this set of equations is solved by a least squares best fit technique. This procedure has the advantage of introducing smoothing into the numerical analysis, and has been adopted as a normal routine. The value of the stress intensity factor is directly proportional to the coefficient of the first term of the series, which is singular and dominates the stress and displacement

fields in the vicinity of the crack tip. Satisfactory convergence of this coefficient is sufficient to obtain the stress intensity factor accurately. Displacements at points not close to the crack tip involve all the coefficients, not equally but with successively diminishing importance. Consequently the analysis must be carried considerably further to obtain satisfactory values of displacements than to obtain the stress intensity factor.

3. FORM AND USE OF RESULTS

The values obtained by boundary collocation of the stress intensity coefficient, $\Gamma = \Gamma(\alpha, \omega) = K_I / (\sigma_P + \sigma_M) \sqrt{a(1 - \alpha)}$, are listed in Table 1; those of the crack mouth displacement coefficient, $\Delta = \Delta(\alpha, \omega) = E'v / (\sigma_P + \sigma_M)a$, are similarly listed in Table 2. As mentioned in the Introduction, these forms of dimensionless coefficient were chosen because of their particular suitability for interpolation over the entire ranges of the two principal dimensionless variables: $\alpha = a/W$, and $\omega = \arctan(\sigma_M/\sigma_P) = \arctan(6M/P(W - a))$. The form of Γ is essentially due to Koiter [4] and [7], and that of Δ is the natural complement. Discussion of the properties and use of these coefficients now follows.

The value of the stress intensity factor, K_I , for any combination of forces is obtained, like a component of stress, by direct superposition. In the present case the value of K_I for the combination of resultant force, P , and couple of moment M is:

$$K = K_P + K_M = (\Gamma_P \sigma_P + \Gamma_M \sigma_M) \sqrt{a(1 - \alpha)} \quad (1)$$

where the subscript I has now been dropped on the understanding that the present context refers exclusively to the first or opening mode of crack extension, and where

$\sigma_P = P/B(W - a)$ is the component of normal net stress due to P

$\sigma_M = 6M/B(W - a)^2$ is the component of normal net stress due to M

$\Gamma_P = K_P/\sigma_P \sqrt{a(1 - \alpha)}$ is the stress intensity coefficient for uniform normal net stress, as given in Table 1 for $\omega = 0$

$\Gamma_M = K_M/\sigma_M \sqrt{a(1 - \alpha)}$ is the stress intensity coefficient for pure bending net stress distribution, as given in Table 1 for $\omega = \pi/2$

The combined stress intensity coefficient is defined as:

$$\Gamma = K / (\sigma_P + \sigma_M) \sqrt{a(1 - \alpha)} \quad (2)$$

$$= (\sigma_P \Gamma_P + \sigma_M \Gamma_M) / (\sigma_P + \sigma_M) \quad (3)$$

$$= (\Gamma_P + \Gamma_M \tan \omega) / (1 + \tan \omega) \quad (4)$$

where $\tan \omega = \sigma_M / \sigma_P = 6M/P(W - a)$

Similarly, for the crack mouth displacement, v :

$$v = v_P + v_M = (\sigma_P \Delta_P + \sigma_M \Delta_M) a / E' \quad (5)$$

where

$$\Delta_P = E' v_P / \sigma_P a$$

$$\Delta_M = E' v_M / \sigma_M a$$

$E' = E$, Young's modulus, for plane stress, or $E/(1 - \nu^2)$ for plane strain, where ν is Poisson's ratio

The effective value of E' for a practical specimen will lie between these limits, and will depend on the ratios a/W and B/W . It is best established by direct experiment on actual specimens or scaled-up models.

Also, the combined crack mouth displacement coefficient is defined as:

$$\Delta = E' v / (\sigma_P + \sigma_M) a \quad (6)$$

$$= (\sigma_P \Delta_P + \sigma_M \Delta_M) / (\sigma_P + \sigma_M) \quad (7)$$

$$= (\Delta_P + \Delta_M \tan \omega) / (1 + \tan \omega) \quad (8)$$

The advantage of the form of the parameter ω is that every possible state of load combination corresponds to one, and only one, value of ω in the range $0 \leq \omega \leq 2\pi$. Figure 3 shows how the four kinds of mixed load combinations might be obtained with a single actuator. Also, eight special cases can be distinguished as follows:

ω	$\tan \omega$	<u>State of load combination</u>
0	0	Simple net tension
$\pi/4$	1	Balanced tension and bending
$\pi/2$	∞	Simple net bending
$3\pi/4$	-1	Balanced bending and compression
π	0	Simple net compression
$5\pi/4$	1	Balanced compression and counterbending
$3\pi/2$	$-\infty$	Simple counterbending
$7\pi/4$	-1	Balanced counterbending and tension

Equations (4) and (8) can be expressed in linear form:

$$\begin{aligned}\Gamma &= (\Gamma_P + \Gamma_M)/2 + (1 - \tan \omega)(\Gamma_P - \Gamma_M)/2(1 + \tan \omega) \\ &= (\Gamma_P + \Gamma_M)/2 + (\Gamma_P - \Gamma_M)\tan(\pi/4 - \omega)/2\end{aligned}\quad (9)$$

$$\Delta = (\Delta_P + \Delta_M)/2 + (\Delta_P - \Delta_M)\tan(\pi/4 - \omega)/2\quad (10)$$

These linear equations enable the results given in Tables 1 and 2, for three values of ω , to be subjected to linear regression analysis, which provides an objective measure of their precision. The sample size of three is minimal, but Eqns. (9) and (10) are true functional relations, not statistical ones, and the three values of the independent variable, $\tan(\pi/4 - \omega) = 1, 0,$ and -1 , are exact; consequently any variation about the regression line is attributable solely to scatter of the boundary collocation values of the dependent variable, Γ or Δ .

The measure of precision calculated was the ratio of the standard error of the estimate to the mean of the three values of the dependent variable, Γ or Δ . The standard error of the estimate is the positive square root of that part of the variance of the dependent variable not accounted for by its regression on the independent variable. The precision of the values of Γ in Table 1 is better than 0.1 percent in all cases. In Table 2 the precision of the values of Δ is also better than 0.1 percent when H/W is 4, but when H/W is 2 or 1 about half of the results are less precise, the worst being hardly better than 1 percent. These less precise results are for $\alpha = 0.1, 0.2, 0.3,$ or 0.8 , not for intermediate values, which reflects the fact that the boundary collocation method is subject to greater round-off errors when the relative crack length is either small or large.

Since both Γ and Δ are linear in the parameter $\tan(\pi/4 - \omega)$, they are linearly related to one another. By elimination of the common parameter in Eqns. (9) and (10):

$$\Gamma = c_1 + c_2 \Delta\quad (11)$$

where:

$$2c_1(\alpha) = \Gamma_P + \Gamma_M - (\Delta_P + \Delta_M)(\Gamma_P - \Gamma_M)/(\Delta_P - \Delta_M)$$

$$c_2(\alpha) = (\Gamma_P - \Gamma_M)/(\Delta_P - \Delta_M)$$

Alternatively, Eqn. (11) can be inverted to give Δ as a linear function of Γ . Either equation can be used in a similar manner to Eqns. (9) and (10) for linear regression analysis. The correlation coefficients for Eqn. (11) were better than 0.99999 in all cases, and the precisions of the regression lines were better than 0.1 percent for $H/W = 4$. It is,

therefore, apparent that the boundary collocation values of Γ and Δ are highly consistent.

There is a further linear relation for the ratio $\Gamma/\Delta = Ka^{1/2}/E'v(1-\alpha)^{1/2}$, which is useful when the crack mouth displacement is the controlled variable in fatigue crack generation or crack extension resistance experiments. Let $v_M/v_P = \tan \theta = (\Delta_M/\Delta_P)\tan \omega$, then it is easily shown that:

$$2(\Gamma/\Delta) = (\Gamma_P/\Delta_P + \Gamma_M/\Delta_M) + (\Gamma_P/\Delta_P - \Gamma_M/\Delta_M)\tan(\pi/4 - \theta) \quad (12)$$

4. END POINT VALUES AND INTERPOLATION EXPRESSIONS

The combined coefficients Γ and Δ are exact functions of the parameter ω by definition - Eqns. (4) and (8) - but the particular coefficients in these equations, namely: $\Gamma_P = \Gamma(\alpha, 0)$, $\Gamma_M = \Gamma(\alpha, \pi/2)$, $\Delta_P = \Delta(\alpha, 0)$ and $\Delta_M = \Delta(\alpha, \pi/2)$, are unknown functions of the parameter α . It is therefore desirable to provide suitable interpolation expressions for these coefficients. These expressions should agree exactly with the end point values of the coefficients at $\alpha = 0$ and 1, which may be assumed to be known very accurately. They should also be acceptably consistent with the end point slopes, $d\Gamma/d\alpha$ and $d\Delta/d\alpha$, though not so stringently as to impose undue complexity on the forms of the interpolation functions. Finally they should agree with the intermediate values of the coefficients, and should not deviate systematically from those values. The intermediate values used in the study of interpolation expressions were those obtained by linear regression analysis of the boundary collocation results for $H/W = 4$, which therefore involve the results for all three values of ω in Tables 1 and 2.

The various end point values are given in Table 3, each with a symbol in parentheses to identify its source. Ten of these values were obtained from either Ref. [2] or [4]. Estimates of the other six were obtained by extrapolation of functions of the variables such that the slopes of the plots were nearly constant near one or the other of the end points. These estimates are identified by the symbol (T) for text. One of them is the coefficient $\Delta(1, 0)$, and its value of -3.26 is estimated to be accurate within about 1 percent. The other five are end point slopes, and may be somewhat less accurate, but are correspondingly less important for the present purpose. It was established that the order of $d\Delta/d\alpha$ at $\alpha = 0$ is $-1/0^{1/2}$ for both values of ω from the fact that plots of Δ against $\alpha^{1/2}$ approach a common slope of -5.4 as α approaches zero.

Interpolation expressions of general conic form which cover the full range of α from 0 to 1 are discussed by Bentham and Koiter in Ref. [4] for the case of Γ_M , and also for the case of uniform tension applied remotely across the gross section, which corresponds in present terms to the combined load case where $\omega = \arctan(3\alpha/(1-\alpha))$. In each case these authors determined the six disposable coefficients of the conic form from

the values of Γ at the end points and those of its first and second derivatives, without recourse to any intermediate values. Since the values of these coefficients are not given in Ref. [4], the present authors determined them from the data of that reference, but found that the resulting expressions were not in sufficiently good agreement with the boundary collocation data. A modified approach was then tried in which only the end point values of Γ and its first derivative were employed, the remaining two conditions required to determine the six coefficients being obtained from the boundary collocation data. This approach was no more successful than the first, so it was concluded that the general conic form was not the most appropriate for the present purpose.

Other forms of interpolation functions are given by Tada et al. in Ref. [2] for both Γ_M and Δ_M , and for the corresponding coefficients for the combined load case of uniform gross tension. These functions, however, do not agree sufficiently well with the present boundary collocation results, though they do agree with the less extensive results of Refs. [1] and [8]. Consequently it was considered necessary to explore other forms of interpolation expressions. The most satisfactory interpolation expressions devised were the rational algebraic functions which follow:

$$\Gamma_P = 1.9887 - 1.468 \alpha - 4.76 \alpha(1 - \alpha)/(1 + \alpha)^2 \quad (13)$$

$$\Gamma_M = 1.9887 - 1.326 \alpha - (3.49 - 0.68 \alpha + 1.35 \alpha^2)\alpha(1 - \alpha)/(1 + \alpha)^2 \quad (14)$$

$$\Delta_P = 5.84 - 9.1 \alpha - 4.1 \alpha^{1/2}(1 - \alpha)^{3/2}/(1 + 0.1435 \alpha) \quad (15)$$

$$\Delta_M = 5.84 - 2.3 \alpha - 3.42 \alpha^2 + 2.52 \alpha^3 - 4.1 \alpha^{1/2}(1 - \alpha)^{3/2}/(1 + 0.1435 \alpha) \quad (16)$$

In each of these expressions the leading coefficient is the value of the function for $\alpha = 0$, and the remaining coefficients are related by the value for $\alpha = 1$, so that each expression has four or less independent numerical coefficients to fit eight boundary collocation values. Moreover, Eqns. (13) and (14) are devised to have features in common, as are Eqns. (15) and (16), so that the general interpolation expressions which correspond to Eqns. (4) and (8) each have only five independent numerical coefficients to fit twenty four boundary collocation values (Tables 1 and 2 for $H/W = 4$). The interpolation expressions therefore involve considerable smoothing of the boundary collocation results. For all six expressions the algebraic mean of the deviations of the boundary collocation values is less than 0.1 percent, and the deviations are unsystematic. For Eqns. (4), (13), and (14) the individual deviations are within plus or minus 0.5 percent, except for $\alpha = 0.1$ where the equations overestimate the boundary collocation values by about 1 percent. It is quite possible that these boundary collocation values for such short cracks are

in error to that extent. For Eqns. (8), (15), and (16) the individual deviations are all within plus or minus 1 percent. From these various considerations it is concluded that the interpolation expressions given here are sufficiently precise and reliable for practical purposes.

5. CRACK MOUTH DISPLACEMENT SLOPES

It is sometimes convenient to use separate knife edges, which are attached to the specimen by screws or adhesive, for mounting the clip gage which is used to measure the crack mouth displacement. In such cases it is necessary to know the values of the displacement coefficient Δ_s at some small distance, s , away from the crack mouth. For this reason values of the crack mouth opening slope $d\Delta/dx$ were obtained and are listed in Table 4. The distance x is measured away from the specimen edge along the extension of the crack line. Then, at a position $x = s$, the value of the displacement coefficient $\Delta_s = \Delta_0 + s d\Delta/dx$, where Δ_0 is the value of Δ at the crack mouth as given in Tables 2 and 3, or by Eqns. (8), (15), and (16). In Table 4 the values obtained by boundary collocation, for $\alpha = 0.1$ to 0.8 , are somewhat less accurate than those of the displacement coefficient itself in Table 2. The reason is that to obtain the derivative involves taking the difference between the displacement at the crack mouth and that at some small distance along the crack. The relative error of this difference is likely to be considerably greater than that of either displacement. To obtain the derivatives with substantially greater accuracy would require that the boundary collocation analysis be carried considerably further. This was not considered to be warranted since it should not be necessary for the supplementary term $s d\Delta/dx$ to exceed about one tenth of the principal term Δ_0 . As a practical rule the distance s should not exceed one-tenth of the crack length.

The value in Table 4 for $\alpha = 0$ was obtained by extrapolation of the inverse square roots of the boundary collocation values to their common value. The values for $\alpha = 1$ are the same as the values of Δ_0 because the crack tip and the "hinge point" are then both located at the back surface of the specimen.

6. DISCUSSION

In Refs. [1] and [8] the present authors published stress intensity and crack mouth displacement coefficients, respectively, for side cracked specimens loaded in uniform tension across the gross section. This boundary condition is equivalent to tensile loading through frictionless pins located at mid width, as shown by the inset in Fig. 4, and it involves the relation: $\sigma_M/\sigma_P = \tan \omega = 3\alpha/(1 - \alpha)$. In this figure the straight lines correspond to Eqn. (9) with coefficients obtained from the interpolation expressions, Eqns. (13) and (14). The points marked by circles on this chart are boundary collocation values of Γ for uniform gross tension which are derived either from Ref. [1] or from recent sup-

plementary results. The maximum deviation of any of these points from the corresponding line is less than 1 percent. Thus the earlier results for this special case are in very good agreement with the interpolation expressions presented here.

Figure 4 also illustrates the point that the state of loading for center pin loaded specimens varies from net tension ($\omega = 0$) when $\alpha = 0$ to net bending ($\omega = \pi/2$) when $\alpha = 1$. At $\alpha = 1/4$ the value of ω is $\pi/4$, and the net bending stress is exactly equal to the net tension stress; for greater values of α the bending stress is predominant. Evidently, a face cracked specimen loaded in this manner does not represent the extreme case of a part-through cracked specimen, as has sometimes been mistakenly assumed. For this purpose the specimen would have to be loaded in such a manner as to maintain uniform net tension for all values of α . Alternatively, it might be more practical to load the specimen so as to maintain uniform displacement across the width at some appropriate distance from the crack. These two alternatives are not exactly equivalent, of course, and might produce significantly different test results. This is a matter for further investigation.

Figure 5 is the chart of the crack mouth opening displacement coefficient Δ which corresponds to Fig. 4. The straight lines represent Eqn. (10) and the coefficients are obtained from the interpolation expressions, Eqns. (15) and (16). The circles represent boundary collocation results for uniform gross tension from Ref. [8]. The deviations of these earlier results from the lines are less than 1/2 percent, except at $\alpha = 0.7$ which is 2 percent below the corresponding line. It is notable that these values of Δ for uniform gross tension do not differ greatly from those for net bending ($\tan(\pi/4 - \omega) = -1$), but are in strong contrast to the values for uniform net tension ($\tan(\pi/4 - \omega) = 1$). Whereas the minimum value of Δ for gross section tension is 2.4, at $\alpha = 0.7$, that for net section tension is -3.26, at $\alpha = 1$.

The reason for the rapid decrease of Δ with increase of α under net section tension is that the equivalent combination of force and couple causes counterbending of the two parts of the specimen on either side of the crack, and this counterbending is greater the longer the crack. In consequence, although the crack tip is always opened by this mode of loading (the stress intensity is always positive), the crack mouth displacement is negative when α exceeds about 0.65. In practice the crack is usually simulated by a pointed slot or notch from which extends a short fatigue crack. The slot mouth displacement can therefore be negative. It is important to appreciate, however, that the present results do not apply if there is contact along any part of the crack faces, because this would induce compressive contact stresses which were not imposed in the present boundary collocation analysis. The effect of such contact stresses can be analyzed by various methods if their magnitude and distribution can be determined.

The crack mouth displacement data are needed for several different purposes, such as in the procedure of ASTM Standard Method of Test E 399

for determination of the K_{IC} plane strain fracture toughness, or for displacement control of fatigue crackling in an electrohydraulic closed loop loading system. Another important purpose, less commonly appreciated, is for analysis of test results when the measured force applied to a cracked specimen is complemented by an unmeasured bending moment. This can occur unintentionally if loading fixtures are designed with insufficient care or appreciation of the nature of the stress distribution imposed on the specimen by the fixture. It will occur when force is transmitted to a face cracked specimen by wedge or hydraulic grips in order to obtain a uniform distribution of end displacement across the specimen width.

The compliance of the specimen, vB/P , can be measured by recording P against v while the specimen is lightly loaded and unloaded. Then, providing that the crack length is accurately known and practically uniform, the value of $\tan \omega$ and thus σ_M can be determined as follows; from Eqn. (6):

$$\begin{aligned} \frac{E'v}{(\sigma_P + \sigma_M)a} &= \Delta(\alpha, \omega) = \frac{\sigma_P \Delta_P(\alpha) + \sigma_M \Delta_M(\alpha)}{(\sigma_P + \sigma_M)} = \frac{E'v}{(1 + \tan \omega)\sigma_P a} \\ &= \frac{\Delta_P + \tan \omega \Delta_M}{1 + \tan \omega} \end{aligned} \quad (17)$$

Hence:

$$\begin{aligned} \tan \omega &= \frac{\sigma_M}{\sigma_P} = \frac{(E'v/\sigma_P a) - \Delta_P}{\Delta_M} \\ &= \frac{(E'Bv/P)(1 - \alpha)/\alpha - \Delta_P}{\Delta_M} \end{aligned} \quad (18)$$

Since the value of α is known, those of Δ_P and Δ_M can be obtained from Eqns. (15) and (16), respectively, vB/P is determined experimentally, so that it only remains to determine the value of E' in order to obtain the value of $\tan \omega$ from Eqn. (18), and hence the value of σ_M . The quantity E' is equal to $E/(1 - x^2)$, where E is Young's modulus and x is equal to 0 for a homogeneous state of generalized plane stress, and is equal to Poisson's ratio for a homogeneous state of plane strain. In practice the values of x for most metallic materials is between 0 and 0.3, depending upon the three parameters: α , ω , and $B/(W - a)$, but independent of size scale. For a given specimen form and material the value of x can be determined from a series of compliance experiments in which the values of α and ω are accurately known. It seems likely that a systematic series of such experiments with several different materials might reveal generalities about the dependence of x on the three dimensionless parameters, and on Poisson's ratio. The authors are not aware of the existence of such information at the present time.

7. SUMMARY

Comprehensive information is presented on the opening mode stress intensity factor, K_I , and on the associated crack mouth displacement, v , for quasi-planar rectangular specimens with single transverse side cracks of any uniform depth, loaded in any manner that can be represented sufficiently well by a linear distribution of normal forces across each end boundary. The data for values of the relative crack length, a , other than the end points, 0 and 1, were obtained by boundary collocation analysis; the end point values were available from the literature, except in one case which was obtained by a reliable method of extrapolation.

The information is given in the form of dimensionless coefficients, $\Gamma(K_I)$ and $\Delta(v)$, which are both functions of two principal dimensionless parameters, a , and the load combination parameter, ω . Both Γ and Δ are linear functions of the quantity $\tan(\pi/4 - \omega)$, and the coefficients of the linear equations are finitely bounded functions of a . Rational algebraic interpolation expressions are given for these functions of a which fit the primary data within the precision of that data, and are considered to be accurate to within 1 percent or better. The effect on Γ and Δ of the third dimensionless parameter, the ratio H/W of half-height to width of the specimen, is shown to be very weak providing that it exceeds unity.

The purpose of the information is to serve as a prerequisite for the development of new test methods for measurement of such properties of materials as fracture toughness, fatigue crack propagation resistance, and stress corrosion crack propagation resistance. The potential advantages of the full range of load combinations (tension or compression combined with bending or counterbending) has by no means been thoroughly explored. Nor has the possibility that the property of interest might be significantly dependent on the mode of loading. This possibility follows from the fact that the characteristics of the crack tip plastic zone will certainly be affected.

APPENDIX: STRESS FUNCTION AND STRESS FUNCTION BOUNDARY CONDITIONS FOR
SIDE CRACKED PLATES

The form of the stress function in terms of the polar coordinates, r and ϕ as shown in Fig. A, is

$$\chi(r, \phi) = \sum_{n=1}^{\infty} r^{n+1/2} A_{2n-1} \left[\cos(n - 3/2)\phi - \left(\frac{2n-3}{2n+1} \right) \cos\left(n + \frac{1}{2}\right)\phi \right] \\ + r^{n+1} A_{2n} [\cos(n-1)\phi - \cos(n+1)\phi] \quad (A1)$$

Its application is discussed in detail in Ref. [3]. The values of the stress function, χ , and its normal derivatives, $\partial\chi/\partial x$ and $\partial\chi/\partial y$, along the prescribed model boundaries (AB, BC, and CD in Fig. A.1 and AB, BB', B'C', C'C, and CD in Fig. A.2) are derived from known boundary tractions as shown in Fig. A, and are as follows:

From the load condition of Fig. A.1 where $P = \sigma_0 BW$ and $M = BW^2 \sigma_0 M/6$.
Along AB

$$\chi = 0 \quad (A2)$$

$$\frac{\partial\chi}{\partial x} = 0 \quad (A3)$$

Along BC

$$\chi = \frac{P}{BW} \left(\frac{x^2}{2} + ax + \frac{a^2}{2} \right) - \frac{12M}{BW^3} \left(\frac{a^3}{6} + \frac{a^2 x}{2} + \frac{ax^2}{2} + \frac{x^3}{6} \right) \\ + \frac{6M}{BW^2} \left(\frac{x^2}{2} + ax + \frac{a^2}{2} \right) \quad (A4)$$

$$\frac{\partial\chi}{\partial y} = 0 \quad (A5)$$

Along CD

$$\chi = \frac{PW}{2B} + \frac{M}{B} \quad (A6)$$

$$\frac{\partial\chi}{\partial x} = \frac{P}{B} \quad (A7)$$

From the load conditions of Fig. A.2 where τ_c and τ_u are the uniformly distributed side shear tractions, we have the following:

Along AB

$$\chi = 0 \quad (A8)$$

$$\frac{\partial \chi}{\partial x} = 0 \quad (A9)$$

Along BB'

$$\chi = 0 \quad (A10)$$

$$\frac{\partial \chi}{\partial x} = \tau_c (y - H) \quad (A11)$$

Along B'C'

$$\chi = \tau_c (V - H)(x + a) \quad (A12)$$

$$\frac{\partial \chi}{\partial y} = 0 \quad (A13)$$

Along C'C

$$\chi = \tau_c (V - H)W \quad (A14)$$

$$\frac{\partial \chi}{\partial x} = \tau_u (V - y) + \tau_c (V - H) \quad (A15)$$

Along CD

$$\chi = \tau_c (V - H)W \quad (A16)$$

$$\frac{\partial \chi}{\partial x} = (\tau_u + \tau_c)(V - H) \quad (A17)$$

REFERENCES

- [1]. B. Gross and J. E. Srawley, "Stress Intensity Factors for Single-Edge Notch Specimens in Bending or Combined Bending and Tension," NASA TN D-2603, National Aeronautics and Space Administration, Jan 1965.
- [2]. H. Tada, P. C. Paris, and G. R. Irwin, "The Stress Analysis of Cracks Handbook," Del Research Corp., Hellertown, Pa., 1973.
- [3]. B. Gross and A. Mendelson, "Elastic Displacements for Various Edge-Crack Plate Specimens," Intern. J. Fracture, Vol. 8, No. 3, Sept. 1972, pp. 267-276.
- [4]. J. T. Bentham and W. T. Koiter, Mechanics of Fracture: I - Methods of Analysis and Solution of Crack Problems, G. C. Sih, ed., Noordhoff Intern. Publ., Leyden, The Netherlands, 1973, pp. 159-162.
- [5]. J. L. Swedlow, ed., The Surface Crack: Physical Problems and Computational Solutions, Am. Soc. Mech. Engrs., New York, 1972.
- [6]. B. Gross, "Some Plane Problem Elastostatic Solutions for Plates Having a V-Notch," NASA TM X-69370, National Aeronautics and Space Administration, Washington, D.C., Jan. 1970.
- [7]. W. T. Koiter, "Stress Intensity Factors for Sheet Strips Under Tensile Loads," Mech. Eng. Lab. Rept. 314, Delft Univ. of Tech. (The Netherlands), 1965.
- [8]. B. Gross, E. Roberts, Jr., and J. E. Srawley, Intern. J. Fracture, vol. 4, No. 3, Sept. 1968, pp. 267-276; Errata, Vol. 6, No. 1, Mar. 1970, p. 87.

Table 1

Boundary collocation values of the stress intensity coefficient Γ obtained with normal traction boundary conditions

H/W	ω	For $\alpha (= a/W)$ values of:							
		0.1	0.2	0.3	0.4	0.5	0.6	0.7	0.8
		$\Gamma = K_I / (\sigma_P + \sigma_M) \sqrt{a(1 - \alpha)}$							
4	0	1.470	1.164	0.961	0.822	0.725	0.659	0.614	0.581
	$\pi/4$	1.528	1.252	1.064	.930	.832	.759	.704	.662
	$\pi/2$	1.585	1.339	1.167	1.039	.938	.858	.794	.743
2	0	1.466	1.164	0.961	0.822	0.725	0.659	0.613	0.580
	$\pi/4$	1.523	1.251	1.064	.930	.832	.758	.704	.661
	$\pi/2$	1.583	1.339	1.167	1.038	.938	.858	.794	.742
1	0	1.468	1.163	0.961	0.822	0.725	0.659	0.614	0.580
	$\pi/4$	1.526	1.250	1.065	.932	.832	.758	.704	.661
	$\pi/2$	1.582	1.338	1.168	1.039	.938	.858	.794	.741

Table 2

Boundary collocation values of the crack mouth opening coefficient Δ obtained with normal traction boundary conditions

H/W	ω	For $\alpha (= a/W)$ values of:							
		0.1	0.2	0.3	0.4	0.5	0.6	0.7	0.8
		$\Delta = E'v / (\sigma_P + \sigma_M)a$							
4	0	3.800	2.770	1.855	1.055	0.331	-0.358	-1.035	-1.730
	$\pi/4$	4.125	3.405	2.763	2.223	1.757	1.335	.934	.540
	$\pi/2$	4.450	4.040	3.670	3.390	3.183	3.027	2.903	2.810
2	0	3.690	2.735	1.850	1.055	0.331	-0.357	-1.037	-1.733
	$\pi/4$	3.985	3.321	2.741	2.220	1.757	1.335	.933	.532
	$\pi/2$	4.400	3.960	3.675	3.381	3.183	3.027	2.901	2.800
1	0	3.860	2.780	1.855	1.055	0.327	-0.367	-1.044	-1.740
	$\pi/4$	4.200	3.420	2.763	2.225	1.763	1.337	.929	.536
	$\pi/2$	4.550	4.060	3.670	3.394	3.190	3.032	2.903	2.795

Table 3

End point values of the coefficients and their derivatives
Sources in parentheses: Refs. [2] or [4] or text (T)

ω	α	Γ	$d\Gamma/d\alpha$	Δ	$d\Delta/d\alpha$
0	0	1.9887 (4)	-6.96 (4)	5.84 (2)	ORDER $(-1/0^{1/2})$ (T)
0	1	.5204 (2)	-0.4 (T)	-3.26 (T)	-9.1 (T)
$\pi/2$	0	1.9887 (4)	-5.40 (4)	5.84 (2)	ORDER $(-1/0^{1/2})$ (T)
$\pi/2$	1	.6629 (4)	-0.332 (4)	2.64 (2)	-1.6 (T)

Table 4

Values of the crack mouth opening slope
 $d\Delta/d(x/W)$

a/W	For ω values of:		
	0	$\pi/4$	$\pi/2$
$d\Delta/d(x/W) = (E'W/\sigma a)dv/dx$			
0	48	48	48
0.1	15.3	18.2	21.1
.2	6.6	9.3	12.0
.3	2.6	5.3	8.0
.4	.44	3.2	6.0
.5	-0.84	2.0	4.9
.6	-1.7	1.2	4.2
.7	-2.3	.63	3.6
.8	-2.9	.27	3.4
.9	-----	-----	-----
1.0	-3.26	-0.31	2.64

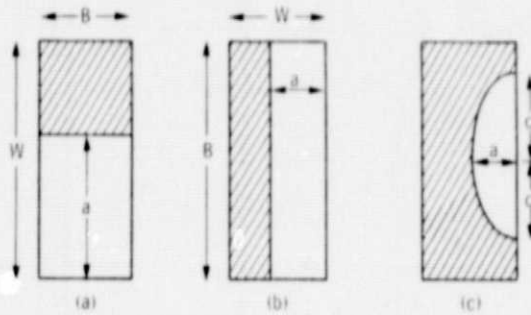


Figure 1. - Cross sections through crack planes of rectangular plate specimens with: (a) edge crack; (b) face crack; (c) part-through semielliptical crack. Note that the width dimension W is always taken to be in the same direction as the crack length a , and the thickness B taken to be normal to that direction.

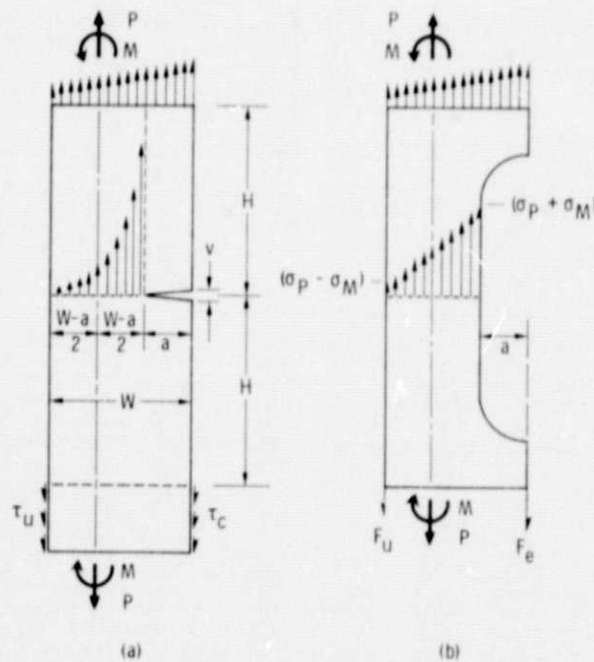


Figure 2. - Specimen model dimensions, equivalent end boundary conditions and stress distributions. (a) Boundary collocation model showing normal tractions case at top and shear tractions case at bottom. (b) Equivalent linear net stress distribution model showing equivalent force pair at bottom.

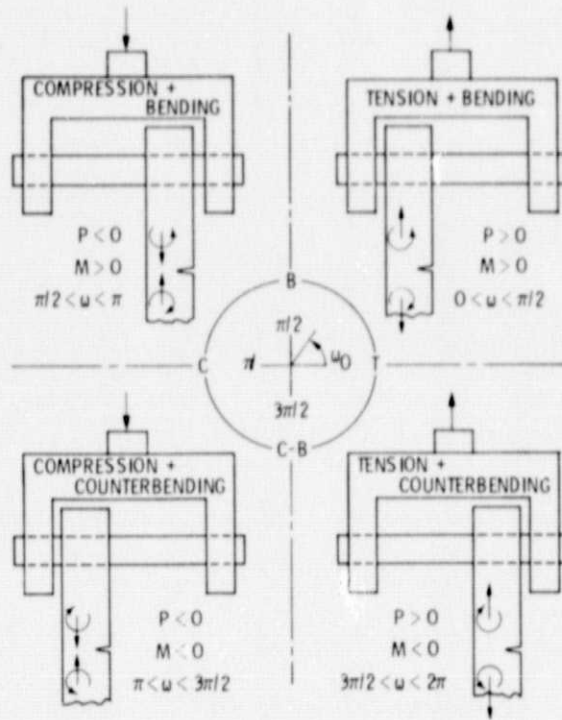


Figure 3. - Illustration of the four kinds of combined load.

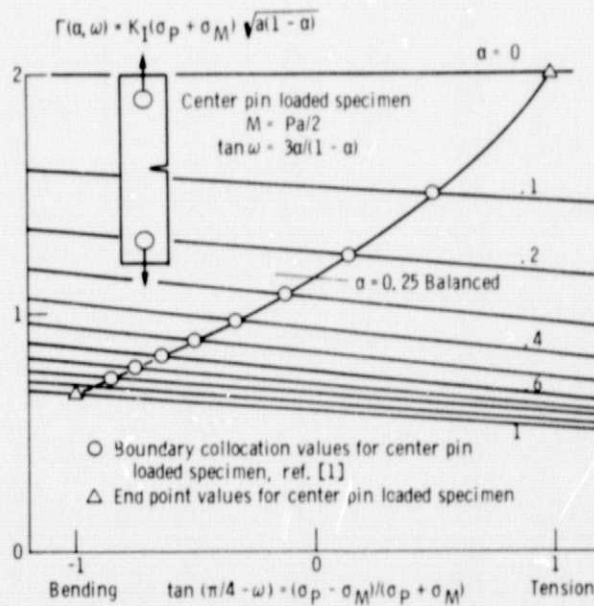


Figure 4. - Stress intensity coefficient, Γ , versus the function $\tan(\pi/4 - \omega)$ of the load combination parameter, ω . The straight lines are the results of the present work for $\omega = 0, \pi/4$, and $\pi/2$. The superimposed points are from earlier work on the case for which $\tan \omega = 3a/(1-a)$.

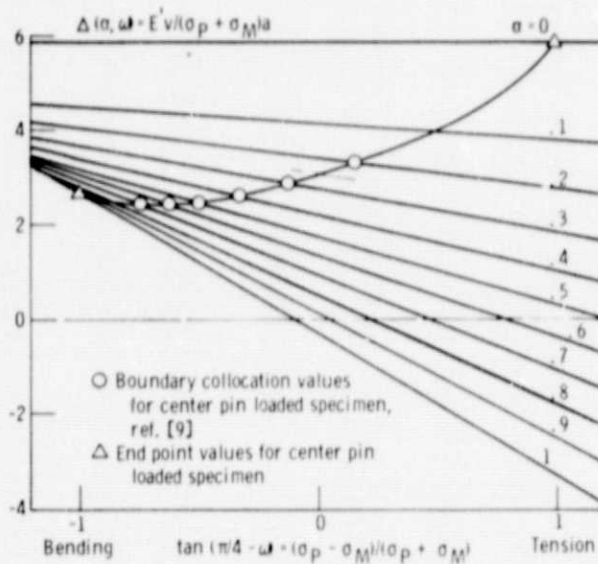


Figure 5. - Crack mouth displacement coefficient, Δ , versus $\tan(\pi/4 - \omega)$. The straight lines are the results of the present work; the superimposed points are from earlier work on the case for which $\tan \omega = 3a/(1 - \alpha)$.

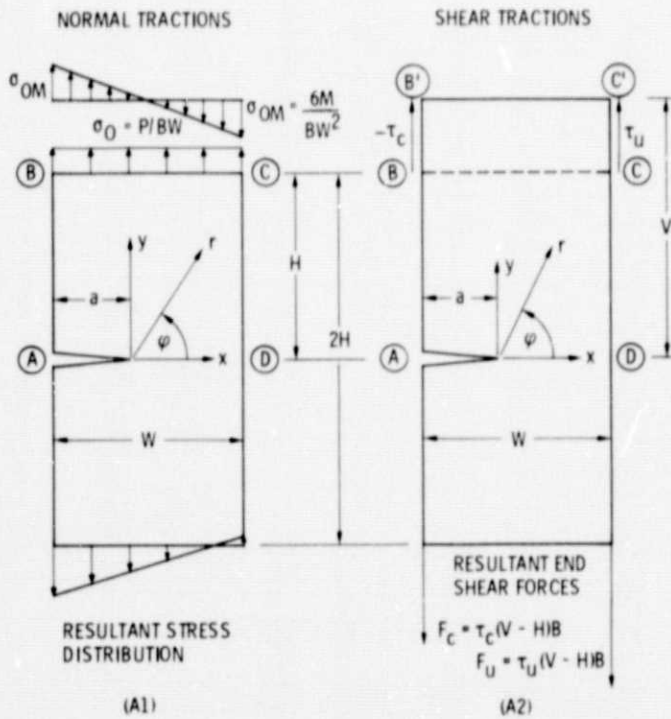


Figure A. - Alternative boundary collocation models.